European Journal of Pharmaceutics and Biopharmaceutics 178 (2022) 117–130

Contents lists available at ScienceDirect

European Journal of Pharmaceutics and Biopharmaceutics

journal homepage: www.elsevier.com/locate/ejpb

A Novel MATLAB®-Algorithm-Based Video Analysis to Quantitatively Determine Solution Creeping in Intact Pharmaceutical Glass Vials

Daniel Molnar [a,1,*], Martina Röhm [a,1], Johannes Wutz [a], Ingrid Rivec [a,b,c], Annika Michel [a,b,c], Gina Klotz [a,d], Jürgen Hubbuch [d], Katharina Schindowski [b], Ingo Presser [a]

[a] Boehringer Ingelheim Pharma GmbH & Co. KG, Formulation and Process Development Biologicals Late Stage, 88397 Biberach, Germany
[b] Institute of Applied Biotechnology, Faculty for Biotechnology, Biberach University of Applied Sciences, 88400 Biberach, Germany
[c] Faculty for Natural Sciences, University of Ulm, Albert-Einstein-Allee 11, 89081 Ulm, Germany
[d] Institute of Process Engineering in Life Sciences, Section IV: Biomolecular Separation Engineering, Karlsruhe Institute of Technology, 76131 Karlsruhe, Germany

ARTICLE INFO

Keywords:
Fogging
Creeping
MATLAB® algorithm
Lyophilisation
Wetting
Contact angle
Polysorbate
Critical micelle concentration
Vial process
Glass vial inner surface

ABSTRACT

During the filling process of a biopharmaceutical drug product (DP), a liquid DP film might creep up the inner vial wall which is barely discernible, appears as milky-white haze after lyophilisation and is known as fogging. Creeping and fogging are mainly dependent on the primary packaging material surface and its hydration, vial preparation process as well as DP composition. The occurrence of both can impede visual inspection and might lead to DP rejection. Hence, our studies focused on the early detection of liquid solution and glass vial surface interaction directly after filling. For a fast and highly sensitive evaluation a novel video-based analysis was used. To our knowledge, this is the first time a MATLAB®-algorithm-based video analysis was applied to quantitatively determine creeping time-resolved. Furthermore, creeping in dependence of vial processing sites, surfactant type and concentration, filling temperature, and vial format were investigated. The results were verified using orthogonal conventional methods such as surface tension, wetting behaviour, and contact angle measurements, as well as ToF-SIMS, ICP-MS, and SEM. Additionally, the methods applied were assessed regarding their cross-validation capability. The observations indicate that the vial preparation process can have a pronounced impact on alteration of the glass vial surface and related creeping behaviour of the filled solution.

1. Introduction

The choice of a suitable primary packaging material is based on the compatibility of the pharmaceutical product, the handling in the production including machinability, distribution of the drug product (DP) and most importantly the patient safety. Generally, glass is the first choice as primary packaging material for biopharmaceutical products due to several advantages. This includes sterilizability, chemical resistance, high impermeability of gas and moisture, as well as simple applicability of the visual inspection due to the transparency of colourless glass [1]. The European Pharmacopeia distinguishes between type I, type II and type III glass containers. Type I glass provides the highest hydrolytic resistance due to the chemical composition of the glass [2]. The higher the hydrolytic resistance of the glass, the higher the quality of the glass, which also results in a lower risk of interaction with the drug product formulation [3]. Another reason for the frequent use of glass containers for parenteral products is the gas tightness protecting the DP from oxidative species such as oxygen, maintaining the sterility and thus avoiding microbial DP contamination [4].

However, contrary to the general assumption that glass is a completely inert material, direct contact of the DP with the inner glass vial wall may lead to reactions such as delamination, fogging or creeping [5,6]. These interactions are mainly driven by the formulation composition and the choice of glass vials [7]. In contrast to glass delamination, which was reported to occur after a certain stability storage period of a liquid drug product, creeping already appears and becomes visible during the vial filling process and is not accompanied with glass detachment. This phenomenon is based on the so-called 'Marangoni Effect' [8,9]. It is described that this Marangoni flow is driven by differences in surface tension of the DP solution and the hydration film located at the inner glass vial wall. This hydration film present at the inner vial surface is caused by environmental conditions such as

* Corresponding author at: Boehringer Ingelheim Pharma GmbH & Co. KG, Birkendorfer Straße 65, 88397 Biberach, Germany.
E-mail address: daniel.molnar@boehringer-ingelheim.com (D. Molnar).
[1] shared first authorship.

https://doi.org/10.1016/j.ejpb.2022.08.003
Received 18 May 2022; Received in revised form 5 August 2022; Accepted 7 August 2022
Available online 9 August 2022

humidity [10]. The liquid meniscus region has a surface tension gradient that is low near the surfactant-rich DP solution surface and high in the hydration film area of the glass (no surfactant present). This causes wetting of the inner glass container walls with a thin DP solution film. The Marangoni effect seems to correlate with the concentration, temperature and the use of surfactants in the formulation [7,11-13]. Creeping becomes visible after lyophilisation in the form of a white, dry, and solid haze or fogging film on the inner glass vial wall. Vial "fogging" can be observed in various irregular random structures such as streaks, fingers, branches, spots or even uniform thin layers [14-17].

As described previously, there are several factors promoting the fogging of a lyophilised DP, such as surfactants [11,12]. However, the surfactant is a mostly inevitable prerequisite in DP formulations to preserve the protein from interface-induced degradation and aggregation by saturation of those interfaces (namely, solid–liquid or air–liquid interfaces) [18-22] and thus, inhibit protein adsorption or protein–-protein self-association [23]. Commonly used surfactants in biopharmaceutical formulations are polysorbate 20 and 80 as well as poloxamer 188 (PS20, PS80, P188) [24]. For antibodies, >70% of the marketed formulations contain either PS20 or PS80 [25]. Nevertheless, although creeping is preferably observed in formulations containing surfactant, the underlying cause can also be found in steps prior to the drug product filling. More specifically, as discussed in literatures, vial sterilization can alter the inner glass vial surface properties and thus creeping [7,13,26,27].

Until today, fogging, the consequence of creeping after lyophilisation, is considered to be only a cosmetic defect, which could complicate the visual inspection. In severe cases of creeping in which the liquid DP formulation reaches the vial opening or stopper sealing area the formerly cosmetic defect might transform into a container closure integrity (CCI) loss [27,28]. However, some questions have remained unanswered. Most importantly, which factors influence the fogging or creeping phenomena to which extent and by what is it caused? What kind of method can be chosen for a direct analysis of an intact vial to evaluate the extent of creeping?

There are different methods available, such as imaging methods including visualization of the wetting behaviour, surface energy measurements, colorimetric staining, scanning electron microscopy (SEM) as well as time-of-flight secondary ion mass spectrometry (ToF-SIMS) and inductively coupled plasma mass spectrometry (ICP-MS) to assess the properties of the glass vial surface. However, until now none of the listed methods enables a quantitative and time-resolved measurement of creeping within the processed and intact vial. For this reason, the purpose of the present study was to develop a novel video-based analysis using a highly sensitive MATLAB® algorithm to quantitively determine the degree of creeping in an intact vial. Hence, it is the first time that the wetting behaviour and therefore, the impact of different vial type and vial preparation sites can be directly assessed and quantified. This enables a fast evaluation of the glass vial surface properties after sterilization and prior to the filling step of the drug product. Moreover, the probability of glass vial fogging of a lyophilised drug product might be reduced or even eliminated by a better understanding of the initial vial material used and vial processing step applied prior to the fill process. Thus, vials sourced from two different sterile vial processing sites, were compared. Additionally, potential influencing factors, such as surface tension, temperature, density, viscosity, filling volume and vial format were evaluated. The surface tension is mainly affected by surfactants. Hence, three different surfactants (PS20, PS80 and P188) were used, the critical micelle concentration (CMC) was determined via surface tension measurement and thus, the optimal surfactant type as well as concentration was identified at which no further surface tension decrease was detected. A defined concentration above the CMC was used to develop and establish the MATLAB®-algorithm-based video analysis. After implementing the video analysis further potential influencing factors, such as surfactant type and concentration, filling temperature, vial process, vial type, and formats were evaluated head-to-head using this novel method. To verify the results gathered via the MATLAB®-algorithm-based video analysis, a well-described, commonly used analytical panel consisting of imaging methods including the wetting behaviour using methylene blue and contact angle measurements of highly purified water in intact vials was applied. Surface energy measurement was performed for surface hydrophobicity determination. Finally, surface morphology and chemical composition were evaluated using SEM, ToF-SIMS and ICP-MS. Additionally, the internally established visualisation of the wetting behaviour using methylene blue solution was also used for cross-validation of the video analysis results. All gathered results were compared to the observations obtained by applying the novel MATLAB®-algorithm-based video analysis to shed light on influencing factors and to evaluate the behaviour of vials sourced from two different sterile manufacturing sites and to broaden process knowledge.

2. Material and methods

2.1. Vial samples

Two different vial types (namely, FIOLAX®, T = TopLyo®, (Schott AG, Mainz, Germany)) and sterile vial processing sites (site A and B) were compared. As internal standard, 20 mL vial formats of FIOLAX® and TopLyo® vials (Schott AG, Mainz, Germany) were used except for the creeping tests where vial formats from 2 mL to 50 mL were included. The unprocessed vials (hereinafter called raw vials) were used as reference sample. The defined nomenclature of the vials obtained from different process steps is shown in Fig. 1. In general, a sterile manufacturing process is divided in a washing and a depyrogenation step. The major differences between the two processes is the temperature applied for depyrogenation (DPY). In sterile manufacturing site A and B, temperatures of $\geq$ 210 °C and $\geq$ 250 °C were applied, respectively. All processed and unprocessed vials were shrink-wrapped in aluminium bags to circumvent an introduction of contaminates by handling and storage.

2.2. Surface tension measurement

Surface tension measurements were performed using a tensiometer DCAT21 and a Wilhelmy-plate (platinum-iridium, PT11) (DataPhysics, Filderstadt, Germany). The measurements were performed at a constant temperature of 20 °C using a sample volume of 20 mL per vessel (inner diameter: 45 mm). For surface tension σ determination, the instrument software DCATS31 (surface/interfacial tension) was applied and calculated according to the Wilhelmy equation [29-31]. By assuming that the Wilhelmy plate is completely wetted with liquid, the equation is simplified and thus, a direct determination of the surface tension by measuring the tension force can be made. All measurements were performed in triplicates.

2.2.1. Critical micelle concentration (CMC) determination

To determine the critical micelle concentration, the surface tension of aqueous solutions with increasing surfactant concentrations of PS 20, PS 80 and P188 (0 – 0.8 mg/mL) (Croda GmbH, Nettetal, Germany) were measured. The determination of the CMC was in accordance with the described procedure [20,32-35]. The measurement was performed in triplicates.

2.3. Density measurement

Density measurements were performed using a density meter DMA 4500 M (Anton Paar GmbH, Graz, Austria) based on the oscillating U-tube principle. The measurement functionality and accuracy were tested via a water test. A sample volume of 1 mL was injected into the measuring cell at 20 °C. The measurement was performed in duplicates.

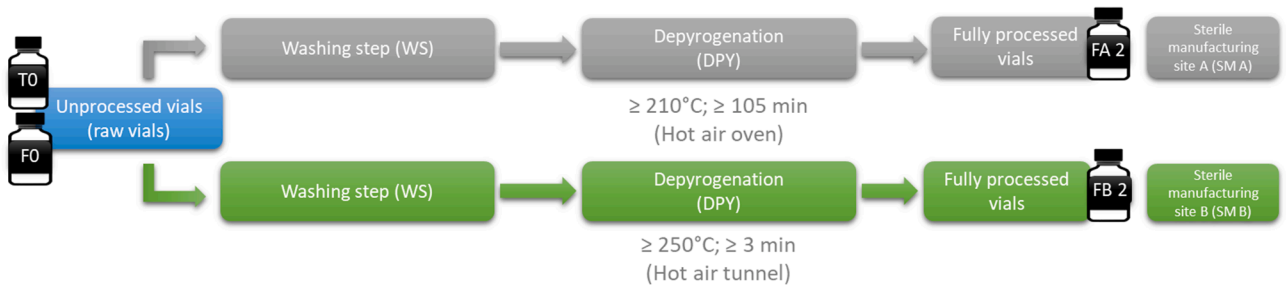

Fig. 1. Flow chart of the different vial process steps. Raw FIOLAX® vials (F0) were processed at sterile manufacturing site A (FA2) and sterile manufacturing site B (FB2). TopLyo® (T0) vials were not processed.

2.4. Viscosity measurement

The dynamic viscosity was measured using a Haake Mars III rheometer (Thermo Fisher Scientific, Langenselbold, Germany). A 35 mm titanium cone with 1° angle was used and the functionality and accuracy were tested by a water test with a zero point adjustment at 20 °C. Subsequently, a sample volume of 210 µL was applied without air inclusions and measured at 20 °C with a shear rate of 1000 s^{-1}. The angular velocity ω of the rotating part gives the shear rate dγ/dt and the applied torque M_d results in the shear stress τ, which led to the calculated viscosity. The measurement was performed in duplicates.

2.5. MATLAB®-algorithm-based video analysis

2.5.1. Evaluation of solution creeping via MATLAB® algorithm

Since pictures or video frames can be treated as matrices containing certain values, it is possible to evaluate them quantitatively by assessing their numeric content (see Fig. 2). Black and white pictures contain grey values, which can be used to evaluate optical changes over time. The evaluation was performed by using a structured (chequered) background and the resulting grey value change caused by the creeping liquid film at the inner vial wall.

First, the width of the glass container was used for the calibration by correlating this metric value to the corresponding number of pixels. Simultaneously, a window was defined for which the evaluation was performed. The top boundary was chosen to exclude the diminution of the bottleneck while the bottom boundary begins just above the liquid level after introducing the liquid (Fig. 2 A). The grey value of the current frame was therefore subtracted from the initial frame and the absolute difference was used for evaluation. Here, a pixel was considered as changed when the difference reaches a certain threshold (Fig. 2 B). The status 'changed' was marked when the film reaches a certain pixel, which effectively enhances the weak signal. The detection of the differences caused increased noise over time, which had to be filtered out by removing single white pixels surrounded by black pixels (Fig. 2 C). The maximal height was detected by adding up the detected pixels over the width of the frame and choosing a certain threshold. The coverage was calculated by a ratio of the overall accumulatively detected pixels and the total amount of pixels in the evaluation window (Fig. 2 D). A brief overview about the subroutines and tools used of the of the MATLAB® algorithm can be found in appendix A.

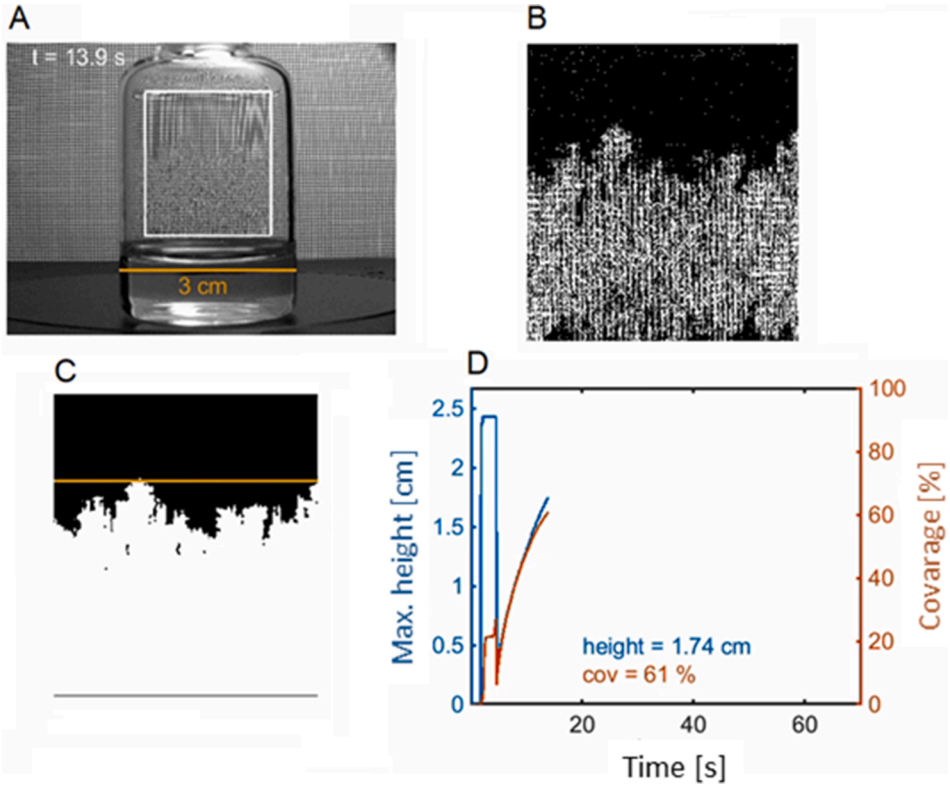

Fig. 2. Procedure of video evaluation of the solution creeping process. A: An original video with the evaluation window (white) and the calibration line (orange) is shown. B: Detected pixels: Difference to the first video frame. C: Pixels that have changed during the measurement after filtering with the maximal height of the liquid film (orange line). D: Maximum height (blue) and coverage (orange) over time. (For interpretation of the references to colour in this figure legend, the reader is referred to the web version of this article.)

2.6. Video analysis and test solutions

The creeping behaviour of the liquid test solution along the inner glass vial wall was determined via video evaluation of the recordings obtained by the digital microscope Keyence VHX 5000 (Keyence Deutschland GmbH, Neu-Isenburg, Germany). The standard settings (vial position, filling volume, filling device (multi stepper pipette (Eppendorf, Hamburg, Germany)), magnification, background, illumination, aperture, distance of the lens to the vial) were kept constant and focus was set manually. The vials were filled with 5 mL test solution at 20 ± 2 °C and recorded for min. 60 s, which was sufficient to ensure that the asymptotical approximation of the signal ending up in a plateau was covered. The plateau indicates the end of the creeping process. However, for evaluation proposes, a timeframe of 40 s is displayed for each sample measured. Various conditions were tested including (i) three surfactant solutions (0.2 mg/mL polysorbate 20, polysorbate 80 and poloxamer 188), (ii) a PS20 concentration series (0.00625 – 0.2 mg/mL), (iii) different temperatures of PS20 solutions (10 °C, 20 °C, 30 °C and 40 °C), (iv) vial processing (F0, FA2, FB2 and T0), (v) vial format (2 mL, 6 mL, 10 mL, 20 mL and 50 mL) and vial path length (20 mL and 30 mL). The measurement was performed in triplicates.

2.7. Visualization of the wetting behaviour using methylene blue solution

For photographic evaluation of the wetting behaviour, a 0.5 mg/mL aqueous methylene blue (Sigma-Aldrich®, St. Quentin Fallavier, France) solution was used to intensify the contrast compared to purified water. It is known from literature that methylene blue is a cationic dye, which might interact with the glass network ions, such as sodium (Na^+) or hydronium (H_3O^+) [36] and that it can be used for colorimetric staining to visualize differences and changes in the surface roughness and morphology [37]. However, within our study, it was not used to identify corroded glass sections on the inner glass surface but as a contrast intensifying agent to better evaluate the filling behaviour of an aqueous methylene blue solution. Thus, four filling volumes (200 µL, 1000 µL, 2000 µL and 5000 µL) were chosen and filled in a 20 mL vial to compare the dependency of vial wetting and degree of vial bottom coverage.

2.8. Contact angle measurement in intact vials

The contact angle was determined at the three-phase point (solid/liquid/gas) using a VHX 5000 microscope (Keyence GmbH, Neu-Isenburg, Germany) at the vial bottom and the inner vial wall using a volume of 5 µL purified water each [38]. To minimize preparation time and the risk of contamination during glass vial breakage or cutting, a head-to-head comparison of broken versus intact glass vials was conducted using two different camera angles (90° and 86°, respectively). The contact angle of an aqueous fluorescein (5 mg/mL and 20 mg/mL) (Sigma-Aldrich®, Steinheim, Germany), methylene blue solution (0.5 mg/mL) and water in intact T0, F0, FA2, FB2 vials were determined. The measurement was performed in triplicates.

2.9. Surface energy measurement

The surface energy of the inner glass vial wall was determined qualitatively using test inks with defined surface energies (Arcotest, Moensheim, Germany) in the range of (i) 28 – 60 mN/m and (ii) 18 – 22 mN/m as well as (iii) 62 – 68 mN/m according to [27]. The test inks were transferred to the inner vial surface using a brush starting with the highest surface energy. If the ink streak on the glass surface remained unchanged after 4 s, the surface energy range was confirmed, whereas a spread of the ink was followed by an iteratively adjustment of the surface energy by 2 mN/m ($s_{Surface} < s_{Ink}$) using different inks according to [27].

2.10. Scanning electron microscopy (SEM)

Scanning electron microscopy (SEM) was performed under vacuum, using an accelerating voltage of 1 keV by SEM Supra 55VP (Zeiss, Oberkochen, Germany) to characterize the morphology of the glass vial bottom and wall in accordance to [5]. Images were loaded with Scan Speed 6 with a cycle time of 1.4 min. The entire glass vial fragments were scanned and images with an aperture of 10 µm and a magnification of 500 × and 5000 × were taken of five independent vial samples.

2.11. Time-of-flight secondary ion mass spectrometry (ToF-SIMS)

ToF-SIMS was performed with a ToF-SIMS-IV-100 (ION-TOF GmbH, Muenster, Germany) and was executed by SCHOTT pharma services (Mainz, Germany) to analyse the first three monolayers in glass vials. The differently processed glass vials were broken and used without any further preparation for the analysis. The test areas implied the inner vial wall directly above the bottom and below the vial shoulder and was performed with a single sample.

2.12. Inductively coupled plasma mass spectrometry (ICP-MS)

For ICP-MS measurements, the vials were filled with purified water (18 mL in 20 mL vials), sealed with cleaned aluminium foil (rinsed with purified water) and subsequently, autoclaved (60 min ≥ 121 °C). After the treatment, the test solution was filled in perfluoro alkoxy polymer (PFA) vessels and analysed via a mass spectrometer 7800 (Agilent GmbH, Frankfurt, Germany). The quantitative method was used for boron, sodium, aluminium and calcium, while the semi-quantitative method was used for silicon determination. The measurements were performed in duplicates.

3. Results

3.1. Surface tension measurements

The occurrence of creeping is facilitated in the presence of a surfactant due to its characteristics in lowering the contact angle and hence, its wetting to hydrophilic surfaces. Thus, prior to develop and implement the MATLAB®-algorithm-based video analysis, the optimal surfactant concentration to achieve maximal surface tension decrease and thus strongly pronounced creeping was determined by surface tension measurements. Hence, the critical micelle concentration (CMC) was determined using different surfactants (polysorbate 20 (PS20) and PS80 as well as poloxamer 188 (P188)) with increasing concentrations in the range of 0 – 0.8 mg/mL. To exclude a possible effect on the wetting caused by the viscosity and density, these two parameters were monitored for the different solutions, accordingly. The viscosity varied negligible (from 1.02 mPa*s to 1.09 mPa*s) and the density remained unchanged for all solutions (0.998 g/cm^3), whereas the surface tension decreased with increasing surfactant concentration. For PS20 it changed from 72.6 mN/m to 38.5 mN/m, for PS80 from 73.5 mN/m to 42.8 mN/m and for P188 from 72.5 mN/m to 53.0 mN/m (see Fig. 3). The CMC is characterized by a strong surface tension decrease with increasing surfactant concentrations.

3.1.1. Determination of the critical micelle concentration (CMC)

The CMC was determined by applying the regression line method according to [20,32-35]. Using this approach, first, the arithmetic average was calculated. The standard deviation was added to the arithmetic average as a worst-case approach to obtain the upper limit of the CMC for each surfactant. Second, a linear fitting was applied for the first and the second line in dependence of a maximal confidence coefficient R^2. The intersection of the two regression lines resulted in the following CMC, 0.011 mg/mL for P188, 0.044 mg/mL for PS80 and 0.099 mg/mL for PS20 and were included in Fig. 3.

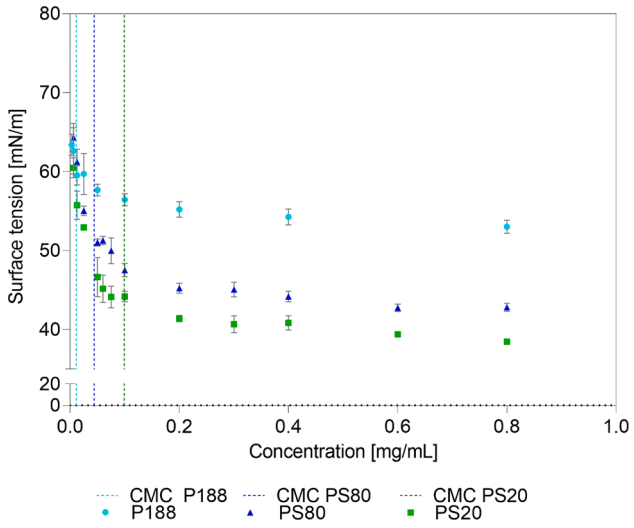

Fig. 3. Surface tension measurement of solutions with different concentrations of PS20, PS80 and P188 (n = 3; mean ± SD). The CMC values (arithmetic average + standard deviation) were determined according to [20,32-35]. The calculated CMC values of PS20 = 0.099 mg/mL (green), PS80 = 0.044 mg/mL (blue) and P188 = 0.011 mg/mL (turquoise) are included within this graph as dotted lines. (For interpretation of the references to colour in this figure legend, the reader is referred to the web version of this article.)

3.1.2. Definition of the optimal surfactant concentration for the subsequent tests

With regard to the investigation of creeping using the MATLAB®-algorithm-based video analysis, a safety factor of minimum two was used to guarantee that the surface tension is within the plateau, remains unchanged (see Fig. 3) and the occurrence of creeping is strongly pronounced. The safety factor of two was applied to the highest CMC determined (namely, the CMC of PS20). Therefore, a pre-set concentration of 0.2 mg/mL for all surfactants was chosen for testing influencing factors towards creeping. In addition to this, this concentration functions as a good reference and is within the concentration range of 0.01 mg/mL to 1 mg/mL which is commonly used for biopharmaceutical drug product formulations [39].

3.1.3. Temperature dependency of the surface tension

A strongly pronounced as well as comparable surface tension decreases of the PS20 and PS80 solutions was observed whereas for P188 it was relatively low. Hence, this test was only performed using PS20. To evaluate the impact of temperature on the creeping behaviour, the temperature of a 0.2 mg/mL PS20 solution was varied from 10 °C to 40 °C. Again, the density, viscosity and surface tension were measured at increased temperatures. The density varied negligible (0.9997 – 0.9923 g/cm^3), whereas the viscosity (1.38 – 0.68 mPa*s) and surface tension decreased ($\sigma_{10°C}$ = 41.16 ± 0.23387 mN/m – $\sigma_{40°C}$ = 35.84 ± 0.06255 mN/m) with increasing temperature (see Fig. 4). The observed surface tension decrease with increasing temperature is in accordance with [20,35] and is based on an increased dehydration of the surfactant molecule due to thermal fluctuation finally leading to a decrease of CMC and surface tension [35,40].

3.2. Quantitative determination of solution creeping via MATLAB® algorithm

A filling volume of 5 mL in 20 mL vials was used for the experiment because a) it constitutes a worst-case ratio of filling volume to inner glass vial surface and b) it is a commonly used target filling volume for lyophilised DP to obtain a filling height of approximately 1 cm and thus is of practical relevance. To determine factors that influence creeping, parameters, such as (i) surfactant type, (ii) PS20 concentration series, (iii) temperature, (iv) vial samples from two different vial processing sites, (v) vial formats and (vi) vial types (see Fig. 5) were varied. Based on the surface tension studies a surfactant concentration of 0.2 mg/mL was used to investigate on the influence of (i) as well as (iii) to (vi).

The head-to-head comparison of PS20, PS80 and P188 revealed that PS20 and PS80 solutions showed comparable coverage rates and creeping kinetics, which is in accordance with the observed results in the surface tension measurements. However, creeping behaviour differed for P188. Surprisingly, although a tenfold higher surfactant concentration than the CMC of P188 was used, only a coverage of approx. 25% was observed (see Fig. 5, A).

Decreasing PS20 concentration below the determined CMC of 0.099

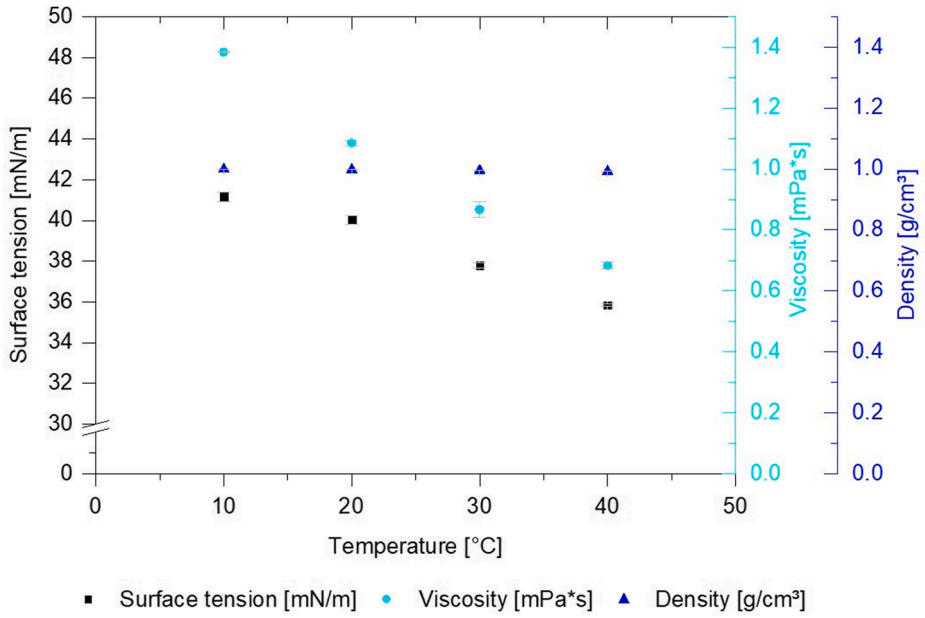

Fig. 4. Surface tension, viscosity and density of differently tempered 0.2 mg/mL PS20 solutions. The dots in black show the surface tension of the respective PS20 concentrations, while the viscosity is presented in turquoise and the density in blue (n = 2; mean ± min and max value). (For interpretation of the references to colour in this figure legend, the reader is referred to the web version of this article.)

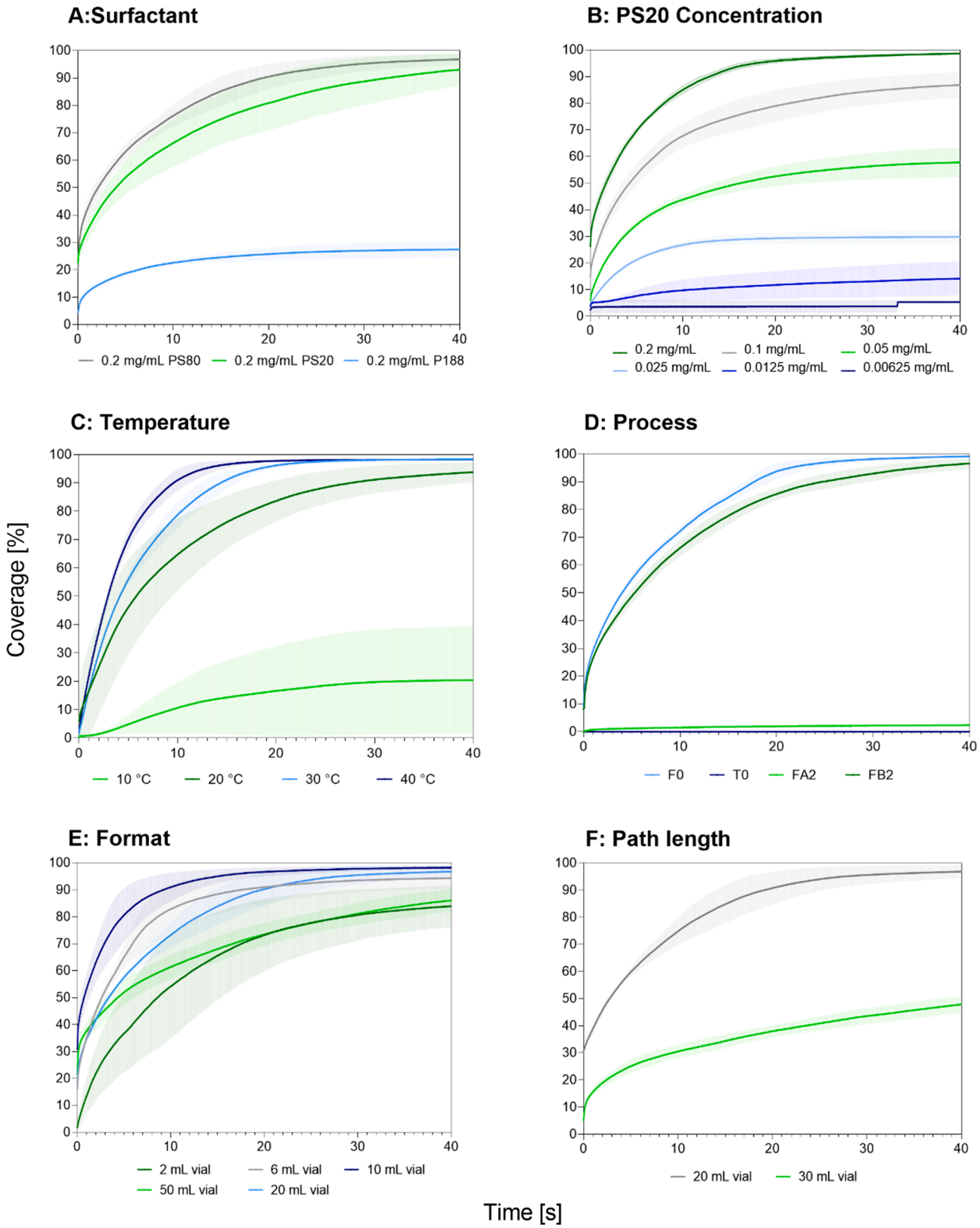

Fig. 5. Solution creeping coverage detection using the MATLAB® algorithm - Impact of the surfactant type, PS20 concentrations, temperature, process, vial format and path length. For A, B, C and D, 20 mL vials with a filling volume of 5 mL were used. In A, the creeping behaviour of the surfactant PS20, PS80 and P188 were investigated. In B, the different PS20 concentrations were tested (0.00625 mg/mL to 0.2 mg/mL). In C, differently tempered (10 °C to 40 °C) solutions with a constant PS20 concentration of 0.2 mg/mL were analysed. In D, variously processed vials from the two sterile manufacturing sites (A and B) were filled with 0.2 mg/mL PS20. In E, the creeping behaviour of different vial formats is shown. In F, the impact of the path length in 20 mL and 30 mL vials (same vial diameter) was evaluated. Unless otherwise stated, a constant PS20 concentration with 0.2 mg/mL in 20 mL FIOLAX® vials was used at 20 °C. The results are shown in triplicates (n = 3, ±SD).

mg/mL did not result in a complete absence of creeping. However, it led to a decreased coverage whereas kinetics was not impacted (see Fig. 5, B). This means, that the CMC cannot be applied as a defined value for the start of creeping but it marks a threshold from which migration of the solution is noticeably different. Hence, the surface tension measurements and the coverage evaluation confirmed that applying a safety margin of two on the CMC of PS20 results in full coverage and a worst-case condition with regard to solution creeping. Due to the comparable behaviour of PS80 and PS20 with respect to creeping kinetics and coverage as well as the confirmed worst-case concentration of 0.2 mg/mL, only PS20 was used as a surrogate for the subsequent MATLAB®-algorithm-based video analysis.

A PS20 solution with a temperature of 10 °C showed a decreased coverage and creeping kinetics, whereas in the temperature range of 20 °C to 40 °C, the total analytical evaluation window was covered and differences were only observed with regard to the kinetics (see Fig. 5 C). Thus, for 0.2 mg/mL PS20 test solutions with a temperature of 10 °C to 40 °C, a positive correlation between temperature and creeping kinetics was observed, which is in line with the decrease of surface tension with increasing temperature.

The 20 mL unprocessed (F0) and processed vials from the two sterile manufacturing sites A (FA2) and B (FB2) revealed different creeping behaviour after being filled with 5 mL of a 0.2 mg/mL PS20 solution (see Fig. 5 D). In hydrophilic unprocessed F0 as well as processed FB2 vials, a complete vial coverage and identical kinetics were observed. On the contrary, for the hydrophilic FA2 vials, no creeping was detected. The results for FA2 vials were in line with the hydrophobic unprocessed TopLyo® (T0) vials. Thus, a dependency of the creeping behaviour on the initial physicochemical composition (F0 versus T0) as well as the vial processing sites (F0, FA2 and FB2) was observed.

In addition, different vial formats were evaluated with regard to solution creeping (see Fig. 5, E). Therefore, the fill volume was adapted for the particular vial type according to the wettable vial inner surface to fill volume ratio of the reference 20 mL vial format. This resulted in a comparable ratio of the wetted vial inner surface between the vial formats. The detection window was adapted for each vial format individually, but the bottom boundary always was the liquid level whereas the top boundary was the vial shoulder. In 2 mL and 50 mL vials, a coverage up to approx. 80% and similar kinetics were observed. In contrast to that, a coverage up to approx. 100% and similar but faster kinetics were measured for 6 mL, 10 mL and 20 mL vials. Thus, a dependency of vial diameter and height was not detected.

To further investigate the dependency of creeping on the distance of filling level to vial shoulder, 20 mL and 30 mL vials with the same diameter but different wall lengths were used. Therefore, the influence of the parameter ′maximal creeping height′ was investigated. The same filling volume of 5.0 mL PS20 solution was taken but the analytical evaluation window height was increased from 2.5 cm to 4.7 cm and the recording time prolonged to 80 s. The PS20 test solution creeped up to 2.9 cm in 30 mL FIOLAX® vials after 80 s, which resulted in a lower overall coverage (see Fig. 5, F) but was higher than 2.5 cm in 20 mL FIOLAX® vials. Considering the fact, that the vial shape was kept constant and only the distance of filling level to shoulder was increased, these results indicate that the test solution would have creeped beyond the analytical evaluation window of 2.5 cm in 20 mL vials. Thus, the vial shoulder area has a suppressive effect on the creeping behaviour. In addition to that, by increasing the distance of filling level to vial shoulder while keeping the filling volume and thus amount of PS20 constant, an incomplete coverage and creeping height was obtained.

In all experiments, no leakage of the test solution or solution creeping beyond the vial shoulder was observed. Therefore, the vial shoulder can be regarded as physical barrier, which has a suppressive effect towards creeping of the solution.

3.3. Visualization of the wetting behaviour using methylene blue solution

To intensify the contrast for photographic evaluation of the wetting behaviour, an aqueous 0.5 mg/mL methylene blue solution (without surfactant) was used. Four different filling volumes (200 µL, 1000 µL, 2000 µL and 5000 µL) were chosen to compare the dependency of the glass vial wetting and degree of glass vial bottom coverage. A difference based on filling volume between wetting behaviour and wettability was observed (see Fig. 6). However, the spreading of the liquid indicated an alteration of the glass vial surface depending on the different sterile vial processing sites. The wettability of the FA2 and T0 vials was poor, and a drop was formed (cohesion > adhesion) at a filling volume of 200 µL. In contrast to that for F0 and FB2 vials a good wettability (cohesion < adhesion) was detected for 200 µL to 5000 µL. However, the wetting behaviour of FA2 and T0 differed for 1000 µL to 5000 µL. A volume of 1000 µL methylene blue solution adhered to the FA2 glass vial wall and tended to spread whereas in T0 a drop was detected and spreading was absent. The meniscus of 5000 µL solution in FA2 and T0 differed. In FA2 vials the liquid surface had a concave curvature whereas in T0 vials it was convex. The vials F0 and FB2 showed a strongly pronounced concave liquid surface curvature. These results indicate that wetting of the methylene blue solution changed volume-dependent in FA2 vials. In contrast to that FB2 and F0 behaved very similar. These results also verify the solution creeping coverage measurements (see Fig. 5, D).

3.4. Contact angle measurements - location, measurement settings and dyes

For a more simplified application of the contact angle method, settings such as location and microscope angle were investigated. Furthermore, the influence of methylene blue (0.5 mg/mL) as well as fluorescein (5 mg/mL and 20 mg/mL) as alternative dye towards the contact angle were tested.

The contact angle of intact glass vials can be determined using a microscope angle of 90° but has the drawback of optical distortion. Thus, glass vial fragments were used in accordance to [13]. To circumvent glass vial breakage and hence an increased likeliness of a contamination, the measuring principle was optimized. Therefore, a comparison of the measuring locations was performed at the inner vial bottom and at the inner, intact glass vial walls. To determine the contact angle in intact glass vials, the contact angle was adapted from 90° to 86° to circumvent the optical distortion and thus to enable contact angle measurement directly within intact glass vials. No significant difference was observed when measuring the contact angle of intact glass at 86° and broken glass at 90° (see Fig. 7, A). Hence, it was demonstrated that with an angle of 86° the optical distortion is minimized and the measurement in intact glass vials can be conducted. Consequently, the subsequent measurements were performed using intact glass vials and a camera angle of 86°. Furthermore, the contact angles at the inner, intact glass vial walls were measured and no significant difference was observed (see Fig. 7, B).

In addition, the applicability of fluorescein as an alternative dye for visualization of the wetting behaviour was tested. Therefore, two different concentrations were chosen (5 mg/mL and 20 mg/mL) and compared to the internal standard 0.5 mg/mL methylene blue. To proof the absence of an influence towards the contact angle and thus wetting behaviour, water, methylene blue and fluorescein were compared.

The use of methylene blue (0.5 mg/mL) and fluorescein (20 mg/mL and 5 mg/mL) as a dye did not result in a difference in contact angles (see Fig. 7, C) and were comparable with the reference (water). Thus, the dye can be used interchangeable for visualization purposes of the wetting behaviour.

Overall, the FIOLAX® vials washed and depyrogenated in sterile manufacturing site A (FA2) showed a high contact angle of approximately 50°, whereas FIOLAX® vials washed and depyrogenated in sterile manufacturing site B (FB2) as well as FIOLAX® raw vials (F0)

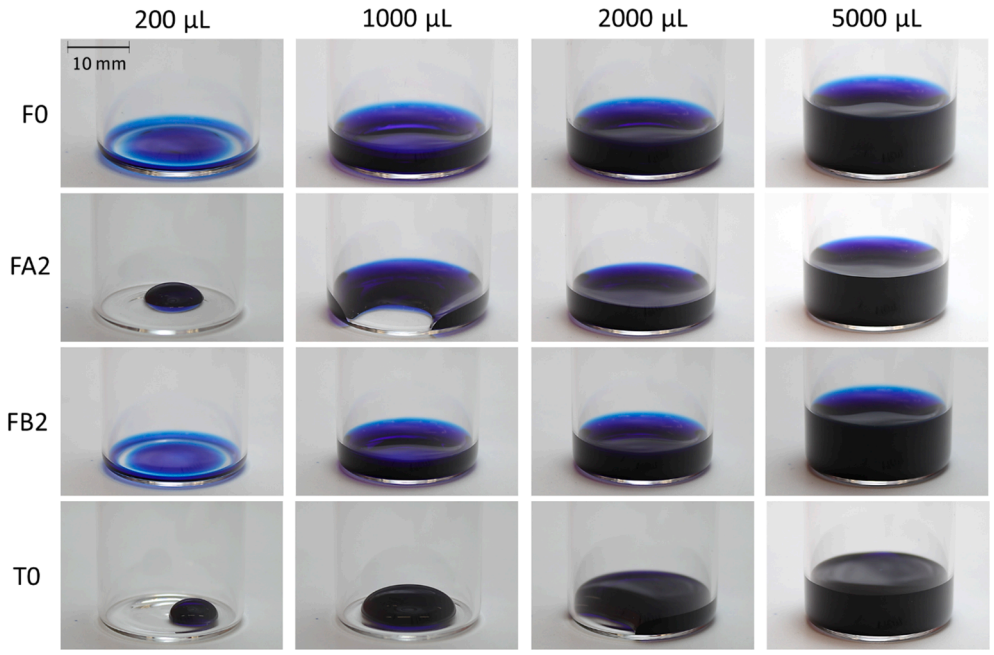

Fig. 6. Wettability dependency of different vials and fill volumes: Raw vials (FIOLAX® (F0) and TopLyo® (T0)) and differently processed vials (FA2, FB2) filled with 200 µL, 1000 µL, 2000 µL and 5000 µL of a 0.5 mg/mL methylene blue solution. Scale bar is 10 mm. (For interpretation of the references to colour in this figure legend, the reader is referred to the web version of this article.)

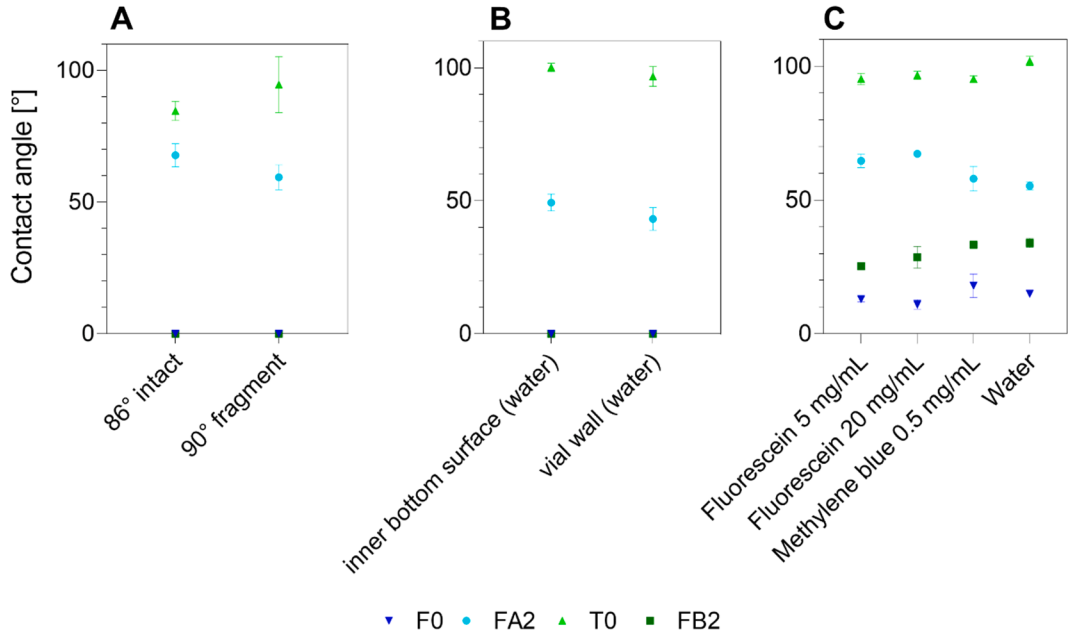

Fig. 7. Contact angle of differently processed vials (F0 = FIOLAX® raw vials; FA2 = FIOLAX® SM A, FB2 = FIOLAX® SM B; T0 = TopLyo® raw vials). In A, the contact angle of an intact (86° measurement angle) and of a broken vial (fragment, 90° measurement angle)) are depicted. In B, the contact angle at different positions (inner bottom surface and vial wall) of the intact vial is shown. In C, the influence of the solution (fluorescein 5 mg/mL and 20 mg/mL, methylene blue 0.5 mg/mL and water) on the contact angle measured in intact vials was evaluated. Values were measured in triplicates (n = 3, mean ± SD). (For interpretation of the references to colour in this figure legend, the reader is referred to the web version of this article.)

showed no contact angle or a contact angle of approximately 10° which marks a threshold regarding evaluability. As a reference, TopLyo® raw vials (T0) were compared and showed the highest contact angle of approx. 100°, which is in line with values known from literature [13,41].

3.5. Surface hydrophobicity measurements via surface energy determination

The surface energy of differently processed vials was investigated using test inks with a defined surface energy. The surface energy determination resulted in a range from 20 mN/m to 66 mN/m, where the samples F0 and FB2 showed the highest surface energy (62 – 64 mN/m). However, the difference in surface energy of differently processed

vials (FA2 and FB2) was not observed within these measurements. Surprisingly, the sample FA2 showed a slightly decreased value of 58 mN/m. The lowest surface energy was observed for the TopLyo® samples T0 with 20 mN/m.

3.6. Surface morphology and chemical composition via SEM, ToF-SIMS and ICP-MS

For the analysis of the surface structure via SEM, the following vial types were analysed: F0 = FIOLAX® raw vials, FA2 = full processed vials in the sterile manufacturing site A (SM A) FIOLAX® Vials, FB2 = full processed vials in the sterile manufacturing site B (SM B). T0 = TopLyo® raw vials. Five vials per vial type were scanned at the bottom and wall area at different magnifications (see Fig. 8). In all vials, the vial bottom surface topography had a uniform pattern at a 500-fold and 5000-fold magnification (data not shown). In the wall area of raw vials, uneven, equally distributed structures were observed, which appeared as round bumps with a diameter of 0.2 µm to 4 µm. This observation was made in all raw vials measured. All fully processed vials from SM A (FA2) showed flat structures at the inner vial wall in the form of circular pits with a diameter of 0.1 µm to 1 µm. The surfaces of the fully processed vials from SM B (FB2) showed similar structures in the form of circular flat bumps with a diameter in the range of 0.5 µm to 1 µm. According to information of the vial manufacturer, the circular structures in the form of bubbles detected at the inner vial wall of raw vials are inorganic process related residuals (silicon borates), which are washed out during vial processing (washing and depyrogenation) and thus appear as flat bumps at the same area. This phenomenon was observed at the inner vial wall for the fully processed vials SM A and SM B in the same manner (namely, occurrence and size). However, the vial bottom remained smooth, and no alteration was detected for any vial type. Thus, it can be concluded that the vial surface was similar after applying two different vial processes and no difference was detected via SEM picture evaluation. The hydrophobic TopLyo® raw vials T0 always used as reference

A: SEM

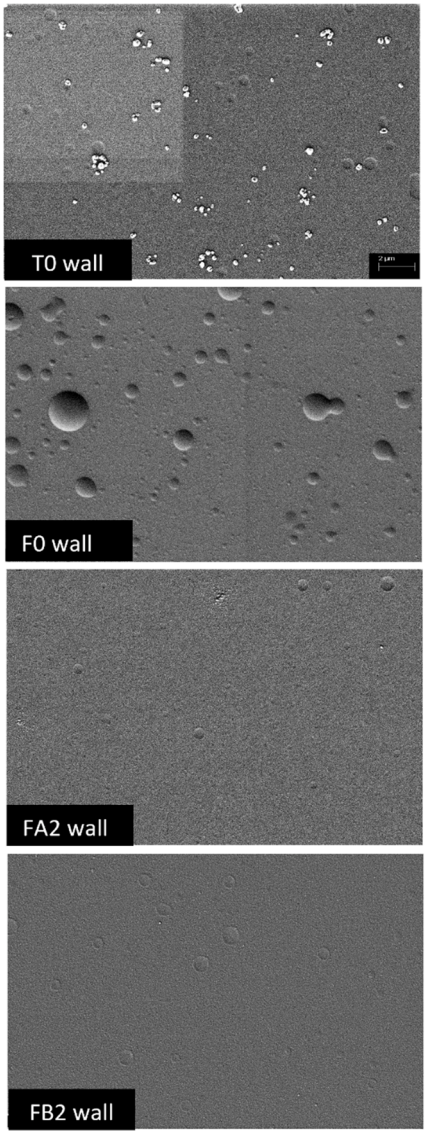

B: ToF-SIMS

Ions	m/z	Intensity T0	F0	FA2	FB2
Na^+	23	n.a.	5985406	3210049	5113354
		n.a.	5839043	3784792	5447712
$(CH_3)_3Si^+$	73	324804	n.a.	24359	5923
		1949	52	20404	7702
$Si_2C_5H_{15}O^+$	147	35326	n.a.	n.a.	n.a.
		n.a.	n.a.	n.a.	51
$C_8H_5O_3^+$	149	2282	n.a.	556	1857
		n.a.	n.a.	878	4233
O^-	16	1066584	5559857	4449651	4550375
		990811	5457299	4158599	4732467
OH^-	17	579902	2047569	1488111	1915206
		536409	1987453	1361008	1813736
$Si_2O_5H^-$	137	n.a.	2762	2622	3511
		n.a.	3828	2899	3847

n.a. = not applicable

C: ICP-MS

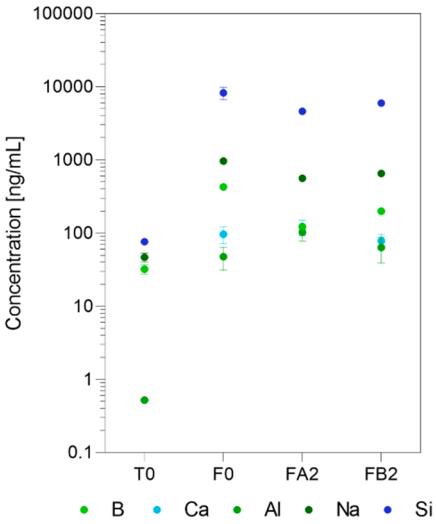

Fig. 8. Surface morphology and chemical composition of differently processed vials. Raw vials (TopLyo®=T0, FIOLAX = F0) and fully processed vials from sterile manufacturing site A (FA2) or B (FB2). In A, SEM pictures T0, F0, FA2, FB2 are depicted. Scale bars are given in white and resemble 2 µm. In B, ToF SIMS results including the most characteristic elements and molecules. In C, results of the ICP-MS analysis are shown. The following elements were detected: Boron (B), aluminium (Al), sodium (Na), calcium (Ca) and silicon (Si). The concentration is given in nanogram per millilitre and results are shown in duplicates (n = 2 ± min /max value).

were included in surface morphology determination. Beside the bumps that were already observed for FIOLAX® vials, an additional structure with uneven arranged bubbles (size range 0.05 µm to 4 µm) was detected.

For chemical characterization of the inner vial wall surface, vials from the same collective were analysed using ToF-SIMS (namely, F0, T0, FA2, FB2). In Fig. 8 B, the peak area for different mass to charge ratios (m/z) is depicted for the samples measured. The spectra of all samples showed a strongly increased positive peak area at $m/z = 23$ and in the same manner a negative peak at $m/z = 16$ as well as an increased negative peak area for $m/z = 17$. Differences for positive peak areas were also measured for $m/z = 72$, 147 and 149 as well as for the negative peak area of $m/z = 137$. The results were compared to a reference material data base of the glass vial manufacturer [42]. After data evaluation, the peaks were assigned to the following glass matrix substances: Na+ ($m/z = 23$), O- ($m/z = 16$), OH– ($m/z = 17$), Si_2O_5H- ($m/z = 137$). Typical elements of the glass such as Na^+, O^- und OH^- are most prominent in sample F0. The results indicate that after washing and depyrogenating in SM A and SM B, the amount of Na^+, O^- und OH^- was reduced in a similar manner independent of respective vial processing procedure.

Besides that, in the samples T0, FA2 and FB2, silicone containing substances ($(CH_3)_3Si^+$ ($m/z = 73$) and $Si_2C_5H_{15}O^+$ ($m/z = 147$)), which are no components of the glass vials were detected. For FA2 vials an increased amount of silicone containing substances ($(CH_3)_3Si^+$ ($m/z = 73$) was detected compared to FB2. This increase in silicone containing substances might lead to glass surface alteration by means of a change in wettability. However, the highest amount was observed for one T0 vial, whereas the second vial contained significantly less. According to information of the manufacturer, the peak for silicon-like structures and the peak for silicone-organic coatings (used for hydrophobisation of the vial) are similar. Thus, it is very likely that the peaks detected for $m/z = 73$ and $m/z = 147$ in T0 raw vials are attributed to the inner vial wall coating.

Moreover, in most of the samples, a peak was detected at $m/z = 149$ ($C_8H_5O3^+$), where FB2 revealed the highest and F0 the lowest peak. According to information of the glass manufacturer, this peak can be attributed to phthalates. Phthalates are commonly used as plasticiser and one source might be the packaging material in which the aluminium shrink-wrapped vials were transported.

Extractable components were investigated using ICP-MS (see Fig. 8, C). For the samples F0, FA2, FB2 and T0, the amount of boron (B), sodium (Na) and silicon (Si) decreased manufacturing site dependent. The boron concentration decreased in the order F0 > FB2 > FA4 > T0. This observation was also made for sodium, where F0 had the highest concentration which decreased by approx. one third for FB2 as well as FA2, respectively. For T0 a marginal amount of sodium was detected. The silicon content was the highest for F0, followed by FB2, and FA2. For T0 a marginal amount of silicon was detected. This means, that during the processing in sterile manufacturing site A and B a washing out of sodium silicone borates for FA2 and FB2 vials did take place. In contrast to that, due to the silicon-organic coating of T0 inner vial surface these glass matrix substances cannot be present and thus detected. The elements aluminium (Al) and calcium (Ca) were detected, but no differences regarding concentration level was observed for F0, FA2 and FB2 vials whereas again in T0 both levels were very low.

This observation is in alignment with the ToF-SIMS results where a decrease in glass matrix substances after vial processing in SM A and SM B was detected.

4. Summary and discussion

A novel high throughput MATLAB®-algorithm-based video analysis was developed and implemented for a time-resolved, quantitative evaluation of processed type I glass vial with regards to the creeping behaviour after the filling of a biopharmaceutical drug product. Various input factors, such as surfactant type and concentration, solution temperature, depyrogenation process, and vial format were investigated. The aim of the study was to determine relevant output parameters for the novel method in relation to known analytical methods. The coverage rate and creeping velocity were identified to be sound output parameters for the extend of creeping and thus a good data basis for evaluation of differently processed type I glass vial as well as determination of influencing factors towards creeping.

To identify a suitable surfactant concentration for evaluating the effect of surfactant type, temperature, vial washing process, vial format, and path lengths towards creeping behaviour, surface tension measurements were performed. Thus, various PS20, PS80 and P188 concentrations were used and ranges in which the surface tension approximated its minimum level (plateau) were identified. The viscosity varied negligible, and the density remained unchanged for all solutions tested. Furthermore, this data were used to determine the critical micelle concentration (CMC) of the respective surfactant according to [20,32-35]. The CMC is influenced by various factors such as surfactant grade and structural properties. We agree with the authors Garidel et al. [20] that a single CMC value can be determined somehow, but due to the complex composition of the surfactants it should be rather seen as a range of CMC values in which micellization takes place [20]. Consequently, the CMC reported in literature differ e.g. for PS20 from 1 µM to approx. 1000 µM [34,43-47]. The CMC of PS20, PS80 and P188 were determined using the tensiometric tangent method [22,41,47]. However, for the sake of simplicity, we referred to upper CMC values when comparing the surfactants PS20, PS80 and P188.

Our results for PS20 and PS80 were in accordance with the observations of Garidel et al. [20], where PS20 resulted in a slightly higher CMC of c = 0.099 mg/mL compared to the CMC of PS80 with c = 0.044 mg/mL. For P188, the surfactant behaved different to the polysorbates due to its structural composition. However, the rapid initial surface tension drop resulted in a CMC of 0.011 mg/mL.

For the MATLAB®-algorithm-based video analysis, the PS20, PS80 and P188 concentration used for surfactant type comparison included a safety factor of minimum two times above the highest CMC (namely, c = 0.099 mg/mL) to guarantee that the surface tension is within the plateau, remains unchanged and thus the occurrence of creeping is strongly pronounced. Hence, for the head-to-head comparison of PS20, PS80 and P188 using the MATLAB®-algorithm-based video analysis, a surfactant concentration of 0.2 mg/mL (approx. two times the CMC of PS20, four times the CMC of PS80 and ten times the CMC of P188) was used.

Maximum creeping coverage was observed for PS20 and PS80. Further, the creeping kinetics only negligibly differed for both surfactant types. This means that the maximum coverage was reached slightly faster for 0.2 mg/mL PS80 solution than for PS20. This behaviour is very likely attributed to the difference in the composition of the fatty acid residuals, i.e. in the hydrophilic-lipophilic balance (HLB) (HLB_{PS20} = 16.7, HLB_{PS80} = 15.0 [48]). These slight differences also detected in CMC for PS80 and PS20, might finally have led to a difference in creeping velocity. However, PS20 and PS80 solutions creeped up the inner vial wall and both led to total coverage of the measurement window. Thus, the results can be regarded as comparable because only marginal differences were observed. Hence, a PS20 concentration of 0.2 mg/mL was chosen due to its practical relevance as it is frequently used in clinical and marketed biopharmaceutical medicinal products. At this concentration, the extent of creeping reached a maximum (up to the vial shoulder area) and represents a worst-case scenario. Moreover, in contrast to PS20 and PS80, the coverage as well as creeping velocity was less pronounced for 0.2 mg/mL P188 and approximated only around 25% even though the surfactant concentration used was ten times the CMC of P188. The decrease in surface tension of P188 measured via tensiometer was also lower compared to the PS20 and PS80 solutions. These results indicate that the surface tension decrease might function as indicator for the resulting coverage. However, the surface tension

decrease alone cannot be exclusively seen as standalone characteristic influencing factor towards creeping but also differences in chemical structure of the surfactant molecule.

As aforementioned only PS20 was used for the subsequent tests due to its comparable behaviour to PS80 regarding kinetics and total vial coverage. To verify if creeping is exclusively dependent on the CMC, increasing PS20 concentrations were filled into FIOLAX® raw vials and analysed using the MATLAB®-algorithm-based video analysis. A correlation between surface tension, CMC, coverage and creeping height was observed. A PS20 concentration above 0.05 mg/mL PS20 resulted in a coverage $>$ 50 % and at the same time the surface tension decreased from approx. 74 mN/m to $<$ 45 mN/m. The kinetics within the measurements remained unaffected. This means, that the CMC cannot be considered as threshold under which creeping is absent, but it marks a point within an interval from which migration of the solution is noticeably different. This hypothesis is supported by the observations made at the CMC of PS20 (CMC = 0.099 mg/mL) where the coverage was approximating 90% but not 100%. A practically relevant and commonly used PS20 concentration (0.2 mg/mL) in biopharmaceuticals led to a coverage of 100%. However, it is described in literature that the presence of an antibody can significantly increase the apparent CMC of the protein-PS20 mixture compared to a protein-free PS20-solution [49]. Mahler et al. observed a fourfold increase in the apparent CMC from approx. 0.1 mg/mL to approx. 0.4 mg/mL after increasing the protein concentration from 10 mg/mL to 150 mg/mL. Hence, in theory (but very unlikely), in case the viscosity of the protein solution would remain unaffected after increasing the protein concentration up to 150 mg/mL, the change in the apparent CMC of the solution would result in a considerably decrease in solution creeping in the glass vials.

Within our studies it was demonstrated that the developed, fast and straightforward method to determine the extent of creeping as well as velocity can be performed in a reproducible way. After implementation and standardization of this valuable tool it was used to evaluate different vial processing sites regarding the likeliness of the occurrence of creeping or to additionally investigate formulation parameters that do have an influence towards it. Thus, it was used to investigate on and to identify potential influencing factors towards creeping.

The temperature of a 0.2 mg/mL PS20 solution was varied from 10 °C to 40 °C to evaluate its impact on the surface tension while monitoring the density and viscosity. The temperature affected the surface tension within a narrow range of $\sigma_{10°C} = 41.2 \pm 0.23$ mN/m to $\sigma_{40°C} = 35.8 \pm 0.063$ mN/m. The observed surface tension decrease with increasing temperature is in accordance to [35,40] and is based on an increased dehydration of the surfactant molecule due to thermal fluctuation finally leading to a decrease of CMC and surface tension [50,51]. The anti-correlation of viscosity and temperature is most likely due to increased thermal energy in the system, increased molecular velocity of individual molecules and thus, a decreased molecular interaction of molecules. This observation is most likely attributed to the surfactant concentration used within our study as the reported viscosity increase was only true for higher surfactant concentrations [51]. In contrast to this, in literature it is also described that non-ionic ethoxylated surfactant solutions show an increase in viscosity with increasing temperature which again is due to dehydration of the non-ionic polar groups [50-52]. However, the reason for the decreased viscosity with increasing solution temperature detected most likely is attributed to the low surfactant concentration used within our study as the reported viscosity increase was again only true for higher surfactant concentrations [51].

The results described above indicate that viscosity had the biggest impact on creeping behaviour. In a temperature range of 10 °C to 20 °C, the viscosity decreased from 1.38 mPa*s to 1.02 mPa*s whereas the coverage rate increased from approx. 20% to 90%. The slight increase in coverage rate but accelerated kinetics observed at a higher surfactant temperature might be explained by a decrease in surface tension in combination with a lower viscosity.

For protein containing solutions the dependency of creeping and viscosity is of importance as well. It is known from literature that with an increasing antibody concentration ($\geq$50 mg/mL) a shift in viscosity towards higher values can be observed [53-57]. In turn, this increase in viscosity could lead to a less pronounced solution creeping. Furthermore, it was demonstrated by Woldeyes et al. that an increased viscosity due to higher protein concentration could be intensified by lowering the solution temperature. Apart from that, an anti-correlation of viscosity and temperature of antibody solutions is described [57]. Hence, by cooling the antibody solution creeping could be further suppressed. The MATLAB®-algorithm-based video analysis revealed a positive correlation between temperature and creeping (vial coverage) as well as creeping kinetics. A PS20 solution temperature of 10 °C showed a decreased coverage and creeping kinetics, whereas in the temperature range from 20 °C to 40 °C, the whole analytical evaluation window was covered, and differences were only observed regarding the kinetics. These results are in line with the decrease of surface tension with increasing temperature because a decrease in surface tension results in a smaller contact angle, an increased wettability and consequently an intensified wettability.

The creeping height as well as velocity in 20 mL vials was measured via the MATLAB®-algorithm-based video analysis and a 5 mL 0.2 g/L aqueous PS20 test solution. Only minor differences with regard to creeping hight and velocity of FIOLAX® raw vials F0 and FB2 via the MATLAB®-algorithm-based video analysis were detected. The solution creeped within approx. 40 s to the vial shoulder. However, neither wetting of the vial opening nor leakage of the test solution was observed. This behaviour might be attributed to the difference in geometry of the upper part of the glass vials. This hypothesis is supported by the observations made for the 30 mL vial in which creeping was observed when enlarging the pathway length from 2.5 cm to 4.7 cm while keeping the parameters such as filling volume and vial inner diameter constant. Here, the PS20 solution only creeped up 2.9 cm after 80 s. This result indicates that a) the creeping might be dependent on the total amount of PS20 present in the solution and b) the solution would have creeped beyond the shoulder of a 20 mL vial. This means, that the vial shoulder constitutes a physical barrier which has a suppressive effect towards creeping of the solution.

The hydrophobic reference vials T0 showed no creeping as expected and a contact angle of approx. 100° which is in line with earlier reported values [13,41]. No creeping of the test solution was also detected for FA2 which is in line with the contact angle measurements where a contact angle of approx. 50° was detected. Thus, the results indicated that vials sourced from FA2 behaved like hydrophobized T0 vials.

A dependency of the creeping behaviour on the initial physicochemical composition of the vial surface (F0 versus T0) as well as the vial processing sites (FA2 and FB2) was observed using the MATLAB®-algorithm-based video analysis.

The influence of different vial formats regarding creeping was evaluated. Herein, the detection window and fill volume (considering the fill volume to inner glass surface area) was adapted for each vial format individually. In 2 mL and 50 mL vials, a coverage of up to approx. 80% and similar kinetics were observed. In contrast to that, a coverage of up to approx. 100% and similar but higher kinetics were measured for 6 mL, 10 mL and 20 mL vials. Thus, a dependency of vial diameter and height was not detected, and creeping was observed to a high extend in all vial formats.

Various well described and commonly used analytical methods known from literature for the characterization of glass vials were performed to complement and verify the novel MATLAB® algorithm-based video analysis. In particular, the properties of differently processed vials from two sterile manufacturing sites were in the focus of this evaluation. In order to evaluate the impact of the vial preparation procedures in two vial processing lines on the glass vial wetting behaviour, selected methods were further developed.

The determination of the wetting behaviour by measuring the

contact angle in different areas of intact glass vials was compared and no difference between the vial wall and vial bottom was observed. The same was true for broken and intact glass vials. It was demonstrated that by using a camera angle of 86°, the optical distortion can be minimized, and comparable contact angles can be measured. In addition, by performing the measurement in intact glass vials a risk of contamination due to the presence of fractured glass splinter and hence falsification of the measurement is circumvented and the necessity of additional preparational steps minimized. Consequently, the method was further developed and became an easy to use, high-throughput method.

The use of methylene blue (0.5 mg/mL) as well as fluorescein (20 mg/mL and 5 mg/mL) as a staining agent and contrast intensifier did neither result in a significant difference in contact angle nor in surface tension. However, the glass vials washed and depyrogenated at different sterile filling lines differed with respect to the contact angle. The FIOLAX® vials washed and depyrogenated in sterile manufacturing site A (FA2) showed a high contact angle of approx. 50°, whereas FIOLAX® vials washed and depyrogenated at the sterile manufacturing site B (FB2) as well as FIOLAX® raw vials (F0) (reference) showed no contact angle. Surprisingly, the observed behaviour indicated that the FB2 vials are or stayed hydrophilic while the FA2 became hydrophobised. As a control TopLyo® raw vials (T0) (reference) were measured and showed a contact angle of approx. 100° which is in line with the values known from literature [13,41]. The wetting behaviour observed within our study together with the creeping analysis completes the work of Huang et al. were a contact angle of $> 40°$ was defined as a threshold for a strong decrease of the appearance of fogging [13], as well as Langer et al. where creeping finally leads to fogging [27]. Fogging is a dried film at the inner glass vial surface after lyophilisation which might impede visual inspection or cause container closure integrity problems. However, in contrast to Huang et al. where a contact angle of 40.8° was determined for a Type I plus® glass vials, within our tests FIOLAX® vials processed in sterile manufacturing site A showed a contact angle of approx. 50°. Due to that, the results indicate a surface alteration or a possible hydrophobisation.

The visualisation of the wetting behaviour using methylene blue solution revealed differences depending on the filling volume as well as sterile vial processing site. A drop was formed (cohesion > adhesion) after filling 200 µL in FA2 and T0 vials whereas for FB2 and F0 a good wettability (cohesion < adhesion) and spreading was observed for 200 µL to 5000 µL. However, the different wetting behaviour of the "hydrophobised" FA2 FIOLAX® vials and the chemically hydrophobised by plasma impulse chemical vapour deposition (PICVD) TopLyo® T0 reference vials became apparent for a filling volume of 1000 µL to 5000 µL. Within the FA2 vials, increasing test volumes resulted in an adherence of the liquid towards the inner glass vial wall. In contrast to that, in T0 vials, the 1000 µL test solution remained as a single drop in the middle of the glass vial where the test solution cohered. Additionally, the meniscus of the solution in the respective vials differed. In FA2 vials a concave, in T0 vials a convex whereas in F0 and FB2 a strongly pronounced concave liquid surface curvature was detected. The results comply with the contact angle measurements, where a lower contact angle (better wettability) was determined for FA2 vials compared to T0 vials. Furthermore, these results verify the MATLAB®-algorithm-based video analysis data. However, it also demonstrates the benefit of using this straightforward, quick test method to differentiate between a hydrophobic, medium hydrophobic and hydrophilic glass vial inner surface. Thus, this screening method using methylene blue solution constitutes, as simple as it is, a real alternative to the contact angle measurement due to minimized preparational steps necessary.

Surprisingly, even though a difference in wetting behaviour was detected, the surface energy measurement did differ only marginally for FA2 and FB2 FIOLAX® vials (58 mN/m and 64 mN/m, respectively) which is in line for hydrophilic surfaces [27]. In contrast to that, the hydrophobic reference samples T0 had a surface energy of 20 mN/m and 22 mN/m, which is in line with reported values for hydrophobic surfaces [27]. One hypothesis might be, that the residual silicone containing substances present in the FA2 vials could have biased the measurement because in contrast to Langer et al, the glass vials FA2 were not siliconized using a silicone oil emulsion which subsequently is baked in. Nevertheless, the comparable results for FA2 and FB2 FIOLAX® vials is inconclusive thus no differentiation could be made using this method.

The surfaces of the fully processed vials FA2 and FB2 showed similar structures of washed out silicon borates appearing in the form of circular flat bumps with a diameter in the range of 0.5 µm to 1 µm detected via SEM pictures which is in accordance to literature [36]. Despite that, within our study neither bumps nor lens-shaped rings were observed in the vial bottom area which is contrary to the observations of Ditter et al. [26]. However, the glass manufacturer as well as the composition of the glass vials was the same. A possible root cause could be a batch-to-batch variability of the vials.

Furthermore, the ICP-MS measurements are in line with the presence of circular flat bumps and the washing out observations as the boron, sodium and silicon concentration was lower after being processed in the sterile manufacturing site. However, the measured contact angle and creeping behaviour of FA2 and FB2 could not be attributed to the glass vial surface structure. Due to the silicon-organic coating of the inner vial surface of T0 decreased levels of glass matrix substances were detected. A difference was observed for T0 where in addition to the bumps (observed in FA2 and FB2) unevenly arranged bubbles (size range 0.05 µm to 4 µm) were detected. These bubbles might be linked to the PICVD modification applied to obtain a hydrophobisation of the inner glass vial surface. However, it has to be stated that with the methods used this hypothesis could not be proven. Furthermore, the root cause evaluation was not in scope of this work but can be investigated in subsequent studies.

This hypothesis of a possible hydrophobisation of the FA2 in comparison to FB2 vials was supported by the solution creeping evaluation using the MATLAB® algorithm-based video analysis as well as by the ToF-SIMS results in which among glass matrix silicone containing substances ($(CH_3)_3Si^+$ ($m/z = 73$) and $Si_2C_5H_{15}O^+$ ($m/z = 147$)) were detected.

The method ToF-SIMS used within this study was semi-quantitative. Thus, only a relative difference in the amount of these silicone containing substances can be stated. Additionally, it has to be mentioned that the thickness of these residues detected are in the range of several nanometres as only the first few monolayers can be analysed. However, FA2 contained qualitative more silicone-organic substances compared to FB2 which most likely resulted in a (higher) level of hydrophobisation finally leading to a difference in the vial wetting (detected via colorimetric staining and contact angle determination) and creeping behaviour (detected via the developed MATLAB®-algorithm-based video analysis). These substances were most likely introduced during the vial processing step because for F0 (raw vials) only in one vial a negligible amount of the species $m/z = 73$ was detected. Due to the fact, that for the transportation of the vials during the processing moving parts are involved which in most cases are lubricated it might have been that a small portion of lubricant was transferred in the depyrogenation area where it was evaporated, introduced into the vials and condensed on the glass vial surface. This was more pronounced for FA2 vials which were processed using a hot air oven meaning, that the whole batch was incubated for ≥ 105 min. In contrast to that, FB2 vials processed in a hot air tunnel had a contact duration of ≥ 3 min. This could explain the increased amount of these substances found inside the FA2 vials. Thus, the observations made are most likely not connected to the temperature applied during the depyrogenation step as reported in the literature [7,13] but are more likely attributed to the batch vs continuous depyrogenation procedure.

A strongly pronounced difference of silicone-like substances was observed for one T0 vial whereas the second vial contained significantly less. According to information of the manufacturer the peak for silicone-like substances and the peak for silicone-organic coatings (used for

hydrophobisation of the vial) are similar. Thus, it is very likely that the peaks detected for $m/z = 73$ and $m/z = 147$ in T0 raw vials are attributed to the inner vial wall coating. Additionally, structures in the form of uneven arranged bubbles (size range 0.05 μm to 4 μm) were detected by SEM. These bubbles could have been located within the examined area of the ToF-SIMS measurement which is known to be relatively small and the depth lays within the nanometre scale. As a result, these local inhomogeneities can influence the outcome of such measurements, finally leading to an excessive increase of peaks for silicone-like substances/ silicone-organic coatings. Therefore, if such an inhomogeneity was not present in the examined ToF-SIMS area (vial two), consequently the peak for silicone-like substances/ silicon-organic coatings would be significantly lower. Thus, it seems that the presence of the unevenly arranged bubbles might be a reason for the difference in T0 ToF-SIMS results.

5. Conclusion

By implementing this newly developed MATLAB®-algorithm-based video analysis, a novel tool was established which can be used to evaluate the comparability of processes from different sterile manufacturing sites. Additionally, it was demonstrated that it also completes the standard analytical panel known from literature and furthermore helps to evaluate the severity (coverage) of the occurrence of creeping. An inverse correlation between low contact angle, high surface energy and occurrence of creeping was observed for FB2, as expected. However, for FA2, the behaviour differed because a high contact angle, high surface energy but no creeping was detected. This most likely is correlating with the presence of silicone containing substances detected via ToF-SIMS. This means, that the sterile vial processing site A and B were not comparable with regard to wettability of the glass vials and solution creeping within the vials. However, current studies are focussing on the source identification of the silicone containing substances detected via ToF-SIMS.

We clearly could demonstrate the benefit of the MATLAB®-algorithm-based video analysis method to quantitatively determine the wetting kinetics, the extent (coverage) as well as the maximum creeping height. The video analysis helps to gather in-depth insights into influencing factors such as the CMC or solution temperature towards these measured parameters. Therefore, an internal standard method to quantify the creeping and hence, to better understand and evaluate critical process as well as formulation parameters was established. The data gathered using the novel MATLAB®-algorithm-based video analysis tool constitutes a base to be referred to in process risk assessments such as a failure mode and effect analysis (FMEA). Furthermore, it facilitates the down ranking of certain potential critical process parameters on a data instead of an experience basis. It can also be used to find various options to prevent liquid film formation without switching from the standard FIOLAX® vial to another vial type accompanied by a completely new process qualification for the alternative primary packaging material.

Declaration of Competing Interest

The authors declare that they have no known competing financial interests or personal relationships that could have appeared to influence the work reported in this paper.

Acknowledgement

The authors would like to acknowledge J. Hasel, M. Prechtl, B. Gebhard, A. Wittmann, S. Pretzel, J. Wolf, N. Hörberger for excellent technical assistance as well as support. D. Henle and I. Rianasari for spell checking and K. Geh for the excellent review as well as the intense and fruitful discussions.

This research did not receive any specific grant from funding agencies in the public, commercial, or not-for-profit sectors.

Appendix A. Supplementary material

Supplementary data to this article can be found online at https://doi.org/10.1016/j.ejpb.2022.08.003.

References

[1] R.A. Schaut, W.P. Weeks, Historical review of glasses used for parenteral packaging, PDA J. Pharm. Sci. Technol. 71 (2017) 279–296, https://doi.org/10.5731/pdajpst.2016.007377.
[2] European Pharmacopoeia 10.0, 3.2.1. Glass containers for pharmaceutical use (01/2019:30201), Eur. Pharmacopoeia. 10 (2019) 453–459.
[3] P. Richet, R. Conradt, A. Takada, J. Dyon, Encyclopedia of Glass Science, Technology, History, and Culture, in: Encycl. Glas. Sci. Technol. Hist. Cult., 1st ed., John Wiley & Sons, 2021. https://doi.org/10.1002/9781118801017.
[4] R. Mathaes, A. Streubel, Parenteral Container Closure Systems, in (2018:) 191–202, https://doi.org/10.1007/978-3-319-90603-4_8.
[5] R.G. Iacocca, N. Toltl, M. Allgeier, B. Bustard, X. Dong, M. Foubert, J. Hofer, S. Peoples, T. Shelbourn, Factors affecting the chemical durability of glass used in the pharmaceutical industry, AAPS PharmSciTech. 11 (2010) 1340–1349, https://doi.org/10.1208/s12249-010-9506-9.
[6] S.A. Pillai, D. Chobisa, D. Urimi, N. Ravindra, Pharmaceutical glass interactions: A review of possibilities, J. Pharm. Sci. Res. 8 (2016) 103–111.
[7] A.M. Abdul-Fattah, R. Oeschger, H. Roehl, I. Bauer Dauphin, M. Worgull, G. Kallmeyer, H.C. Mahler, Investigating factors leading to fogging of glass vials in lyophilized drug products, Eur. J. Pharm. Biopharm. 85 (2013) 314–326, https://doi.org/10.1016/j.ejpb.2013.06.007.
[8] P.A. Kralchevsky, K.D. Danov, N.D. Denkov, Chemical physics of colloid systems and interfaces, Handb. Surf. Colloid Chem. 2 (1997).
[9] R. Tadmor, Marangoni flow revisited, J. Colloid Interface Sci. 332 (2009) 451–454, https://doi.org/10.1016/j.jcis.2008.12.047.
[10] K. Bange, S. Glas, F. Rauch, Surface hydration of glasses and compositional changes 9 (4) (1999) 17.
[11] S. He, J.B. Ketterson, Surfactant-driven spreading of a liquid on a vertical surface, Phys. Fluids. 7 (1995) 2640–2647, https://doi.org/10.1063/1.868712.
[12] V. Ludviksson, E.N. Lightfoot, The dynamics of thin liquid films in the presence of surface-tension gradients, AIChE J. 17 (1971) 1166–1173, https://doi.org/10.1002/aic.690170523.
[13] M. Huang, E. Childs, K. Roffi, F. Karim, J. Juneau, B. Bhatnagar, S. Tchessalov, Investigation of fogging behavior in a lyophilized drug product, J. Pharm. Sci. 108 (2019) 1101–1109, https://doi.org/10.1016/j.xphs.2018.10.015.
[14] O.K. Matar, S.M. Troian, The development of transient fingering patterns during the spreading of surfactant coated films, Phys. Fluids. 11 (1999) 3232–3246, https://doi.org/10.1063/1.870185.
[15] M.H. Eres, L.W. Schwartz, R.V. Roy, Fingering phenomena for driven coating films, Phys. Fluids. 12 (2000) 1278–1295, https://doi.org/10.1063/1.870382.
[16] A.M. Cazabat, F. Heslot, S.M. Troian, P. Carles, Fingering instability of thin spreading, Nature. 245 (1990) 118–143, https://doi.org/10.1038/346824a0.
[17] A.M. Cazabat, F. Heslot, P. Carles, S.M. Troian, Hydrodynamic fingering instability of driven wetting films, Adv. Colloid Interface Sci. 39 (1992) 61–75, https://doi.org/10.1016/0001-8686(92)80055-3.
[18] M. Rabe, A. Kerth, A. Blume, P. Garidel, Albumin displacement at the air–water interface by Tween (Polysorbate) surfactants, Eur. Biophys. J. 49 (2020) 533–547, https://doi.org/10.1007/s00249-020-01459-4.
[19] J. Li, M.E. Krause, X. Chen, Y. Cheng, W. Dai, J.J. Hill, M. Huang, S. Jordan, D. LaCasse, L. Narhi, E. Shalaev, I.C. Shieh, J.C. Thomas, R. Tu, S. Zheng, L. Zhu, Interfacial stress in the development of biologics: fundamental understanding, current practice, and future perspective, AAPS J. 21 (2019), https://doi.org/10.1208/s12248-019-0312-3.
[20] P. Garidel, M. Blech, J. Buske, A. Blume, Surface Tension and Self-association properties of aqueous Polysorbate 20 HP and 80 HP solutions: insights into protein stabilisation mechanisms, J. Pharm. Innov. 16 (4) (2021) 726–734, https://doi.org/10.1007/s12247-020-09488-4.
[21] A. Arsiccio, R. Pisano, Surfactants as stabilizers for biopharmaceuticals: an insight into the molecular mechanisms for inhibition of protein aggregation, Eur. J. Pharm. Biopharm. 128 (2018) 98–106, https://doi.org/10.1016/j.ejpb.2018.04.005.
[22] A. Arsiccio, J. McCarty, R. Pisano, J.E. Shea, Effect of surfactants on surface-induced denaturation of proteins: evidence of an orientation-dependent mechanism, J. Phys. Chem. B. 122 (2018) 11390–11399, https://doi.org/10.1021/acs.jpcb.8b07368.
[23] B.A. Kerwin, Polysorbates 20 and 80 Used in the formulation of protein biotherapeutics: structure and degradation pathways, J. Pharm. Sci. 97 (2008) 2924–2935, https://doi.org/10.1002/jps.21190.
[24] T.A. Khan, H.C. Mahler, R.S.K. Kishore, Key interactions of surfactants in therapeutic protein formulations: a review, Eur. J. Pharm. Biopharm. 97 (2015) 60–67, https://doi.org/10.1016/j.ejpb.2015.09.016.
[25] R.S.K. Kishore, A. Pappenberger, I.B. Dauphin, A. Ross, B. Buergi, A. Staempfli, H.-C. Mahler, Degradation of Polysorbates 20 and 80: studies on thermal autoxidation and hydrolysis, J. Pharm. Sci. 100 (2011) 721–731, https://doi.org/10.1002/jps.22290.

[26] D. Ditter, H.C. Mahler, L. Gohlke, A. Nieto, H. Roehl, J. Huwyler, M. Wahl, A. Allmendinger, Impact of vial washing and depyrogenation on surface properties and delamination risk of glass vials, Pharm. Res. 35 (2018), https://doi.org/10.1007/s11095-018-2421-6.
[27] C. Langer, H.C. Mahler, A. Koulov, N. Marti, C. Grigore, A. Matter, P. Chalus, S. Singh, T. Lemazurier, S. Joerg, R. Mathaes, Method to predict glass vial fogging in lyophilized drug products, J. Pharm. Sci. 109 (2020) 323–330, https://doi.org/10.1016/j.xphs.2019.08.024.
[28] H. Roehl, P. Lam, D. Ditter, Fogging, in: N.W. Warne, H.-C. Mahler (Eds.), Challenges Protein Prod. Dev., Springer International Publishing, Cham, 2018: pp. 305–309. https://doi.org/10.1007/978-3-319-90603-4_14.
[29] M.J. Schwuger, Lehrbuch der Grenzflächenchemie, Thieme Stuttgart, 1996.
[30] H.-D. Dörfler, Grenzflächen-und Kolloidchemie, VCH, 1994.
[31] G. Brezesinski, H.-J. Mögel, Grenzflächen und Kolloide: physikalisch-chemische Grundlagen; mit 3 Tabellen, Spektrum Akad. Verlag, 1993.
[32] B. Farhadieh, Determination of cmc and partial specific volume of polysorbates 20, 60, and 80 from densities of their aqueous solutions, J. Pharm. Sci. 62 (1973) 1685–1688, https://doi.org/10.1002/jps.2600621022.
[33] S.K. Hait, S.P. Moulik, Determination of Critical Micelle Concentration (CMC) of Nonionic Surfactants by Donor-Acceptor Interaction with Iodine and Correlation of CMC with Hydrophile-Lipophile Balance and Other Parameters of the Surfactants, J. Surfactants Deterg. 4 (2001) 303–309, https://doi.org/10.1007/s11743-001-0184-2.
[34] K.L. Mittal, Determination of CMC of polysorbate 20 in aqueous solution by surface tension method, J. Pharm. Sci. 61 (1972) 1334–1335, https://doi.org/10.1002/jps.2600610842.
[35] M.E. Mahmood, D. a F. Al-koofee, Effect of Temperature Changes on Critical Micelle Concentration for Tween Series Surfactant, Glob. J. Sci. Front. Res. Chem. 13 (2013) 1–7.
[36] D. Ditter, H.C. Mahler, H. Roehl, M. Wahl, J. Huwyler, A. Nieto, A. Allmendinger, Characterization of surface properties of glass vials used as primary packaging material for parenterals, Eur. J. Pharm. Biopharm. 125 (2018) 58–67, https://doi.org/10.1016/j.ejpb.2017.12.018.
[37] D. Ditter, A. Nieto, H.C. Mahler, H. Roehl, M. Wahl, J. Huwyler, A. Allmendinger, Evaluation of glass delamination risk in pharmaceutical 10 mL/10R Vials, J. Pharm. Sci. 107 (2018) 624–637, https://doi.org/10.1016/j.xphs.2017.09.016.
[38] E. Rödel, F. Blatter, J.-P. Büttiker, W. Weirich, H.-C. Mahler, Contact Angle Measurements on Glass Surfaces of Injection Solution Contains / Application of force tensiometry as a tool for contact angle measurement on strongly curved hydrophobic glass surfaces of pharmaceutical packaging containers, Pharm. Ind. 75 (2013) 328–333.
[39] A. Martos, W. Koch, W. Jiskoot, K. Wuchner, G. Winter, W. Friess, A. Hawe, Trends on analytical characterization of polysorbates and their degradation products in biopharmaceutical formulations, J. Pharm. Sci. 106 (2017) 1722–1735, https://doi.org/10.1016/j.xphs.2017.03.001.
[40] E. Mohajeri, G.D. Noudeh, Effect of temperature on the critical micelle concentration and micellization thermodynamic of nonionic surfactants: polyoxyethylene sorbitan fatty acid esters, E-Journal Chem. 9 (2012) 2268–2274, https://doi.org/10.1155/2012/961739.
[41] H. Roehl, P. Lam, D. Ditter, Fogging, in: N.W. Warne, H.-C. Mahler (Eds.), Challenges Protein Prod. Dev., AAPS PharmSciTech, 2018: pp. 305–309. https://doi.org/10.1007/978-3-319-90603-4.
[42] B. Horsfield, F. Leistner, K. Hall, CHAPTER 7 Microscale Sealed Vessel Pyrolysis, in: Princ. Pract. Anal. Tech. Geosci., RSC, 2015: pp. 209–250. https://doi.org/10.1039/9781782625025-00209.
[43] M.C. Ortiz-Tafoya, A. Tecante, Physicochemical characterization of sodium stearoyl lactylate (SSL), polyoxyethylene sorbitan monolaurate (Tween 20) and κ -carrageenan, Data Br. 19 (2018) 642–650, https://doi.org/10.1016/j.dib.2018.05.064.
[44] S. Horiuchi, G. Winter, CMC determination of nonionic surfactants in protein formulations using ultrasonic resonance technology, Eur. J. Pharm. Biopharm. 92 (2015) 8–14, https://doi.org/10.1016/j.ejpb.2015.02.005.
[45] L.S.C. Wan, P.F.S. Lee, CMC of Polysorbates, J. Pharm. Sci. 63 (1974) 136–137, https://doi.org/10.1002/jps.2600630136.
[46] E.S. Basheva, P.A. Kralchevsky, K.D. Danov, K.P. Ananthapadmanabhan, A. Lips, The colloid structural forces as a tool for particle characterization and control of dispersion stability w, Phys. Chem. Chem. Phys. 9 (38) (2007) 5183, https://doi.org/10.1039/B705758J.
[47] N. Rehman, H. Ullah, S. Alam, A.K. Jan, S.W. Khan, M. Tariq, Surface and thermodynamic study of micellization of non ionic surfactant / diblock copolymer system as revealed by surface tension and conductivity, J. Mater. Environ. Sci. 8 (2017) 1161–1167.
[48] X. Guo, Z. Rong, X. Ying, Calculation of hydrophile – lipophile balance for polyethoxylated surfactants by group contribution method, J. Colloid Interface Sci. 298 (2006) 441–450, https://doi.org/10.1016/j.jcis.2005.12.009.
[49] H.-C. Mahler, F. Senner, K. Maeder, R. Mueller, Surface activity of a monoclonal antibody, J. Pharm. Sci. 98 (2009) 4525–4533, https://doi.org/10.1002/jps.21776.
[50] S. Puvvada, D. Blankschtein, Theoretical and experimental investigations of micellar properties of aqueous solutions containing binary mixtures of nonionic surfactants, J. Phys. Chem. 96 (13) (1992) 5579–5592, https://doi.org/10.1021/J100192A071.
[51] E. Constantin, P. Freyssingeas, Oswald, Structural Transition in the Isotropic Phase of the C12EO6/H2O Lyotropic Mixture: a rheological investigation, Langmuir. 19 (2003) 2554–2559, https://doi.org/10.1021/la026595o.
[52] C. Mesa, G. Risuleo, Surfactant Mixtures: Performances vs. Aggregation States, in: A. Dutta (Ed.), Surfactants Deterg., IntechOpen, London, 2019: p. 102. https://doi.org/10.5772/intechopen.85437.
[53] S.J. Shire, Z. Shahrokh, J. Liu, Challenges in the development of high protein concentration formulations, J. Pharm. Sci. 93 (2004) 1390–1402, https://doi.org/10.1002/jps.20079.
[54] B.D. Connolly, C. Petry, S. Yadav, B. Demeule, N. Ciaccio, J.M.R. Moore, S.J. Shire, Y.R. Gokarn, Weak interactions govern the viscosity of concentrated antibody solutions: high-throughput analysis using the diffusion interaction parameter, Biophys. J. 103 (2012) 69–78, https://doi.org/10.1016/j.bpj.2012.04.047.
[55] D.S. Tomar, S. Kumar, S.K. Singh, S. Goswami, L. Li, Molecular basis of high viscosity in concentrated antibody solutions: strategies for high concentration drug product development, MAbs. 8 (2016) 216–228, https://doi.org/10.1080/19420862.2015.1128606.
[56] J. Liu, M.D.H. Nguyen, J.D. Andya, S.J. Shire, Reversible self-association increases the viscosity of a concentrated monoclonal antibody in aqueous solution, J. Pharm. Sci. 94 (2005) 1928–1940, https://doi.org/10.1002/jps.20347.
[57] M.A. Woldeyes, W. Qi, V.I. Razinkov, E.M. Furst, C.J. Roberts, Temperature dependence of protein solution viscosity and protein-protein interactions: insights into the origins of high-viscosity protein solutions, Mol. Pharm. 17 (2020) 4473–4482, https://doi.org/10.1021/acs.molpharmaceut.0c00552.